Available online at www.sciencedirect.com

ScienceDirect

Geochimica et Cosmochimica Acta 221 (2018) 145–161

Geochimica et Cosmochimica Acta

www.elsevier.com/locate/gca

Correlated silicon and titanium isotopic compositions of presolar SiC grains from the Murchison CM2 chondrite

Frank Gyngard *, Sachiko Amari, Ernst Zinner [1], Kuljeet Kaur Marhas [2]

Laboratory for Space Sciences and the Department of Physics, Washington University, One Brookings Drive, St. Louis, MO 63130, USA

Received 10 October 2016; accepted in revised form 16 September 2017; available online 23 September 2017

Abstract

We report correlated Si, and Ti isotopic compositions and elemental concentrations of 238 presolar SiC grains from the Murchison CM2 meteorite. Combined with measurements of the C and N isotopic compositions of these 238 grains, 220 were determined to be of type mainstream, 10 type AB, 4 type Y and 4 type Z. SiC grains of diameter $\gtrsim 2.5$ μm, to ensure enough material to attempt Ti measurements, were randomly chosen without any other prejudice. The Ti isotopic compositions of the majority of the grains are characterized by enrichments in ^{46}Ti, ^{47}Ti, ^{49}Ti, and ^{50}Ti relative to ^{48}Ti, and show linear isotopic correlations indicative of galactic chemical evolution and neutron capture of the grains parent stars. The variability in the observed Ti signal as a function of depth in most of the grains indicates the presence of distinct subgrains, likely TiC that have been previously observed in TEM studies. Vandium-51 concentrations correlate with those of Ti, indicating V substitutes for Ti in the TiC matrix in many of the grains. No isotopic anomalies in ^{52}Cr/^{53}Cr ratios were observed, and Cr concentrations did not correlate with those of either Ti or V.

Keywords: Presolar grains; Galactic chemical evolution; Nucleosynthesis; Silicon carbide; NanoSIMS; Asymptotic branch stars

1. INTRODUCTION

Meteorites, or colloquially "rocks from space", are a multi-variate agglomeration of minerals and dust sourced from a variety of astrophysical bodies. While some space rocks are certainly cometary, lunar, or Martian in origin, the vast majority originate from the asteroid belt – the debris of asteroidal collisions that by happenstance made its way to Earth and survived atmospheric melting. The isotopic composition of the most primitive components of these rocks, specifically Ca-Al-rich inclusions (e.g., Jacobsen et al., 2008), is the foundation upon which the age of the Solar System is determined. Additionally, the elemental compositions of carbonaceous chondritic meteorites form the basis of the primordial, undifferentiated composition of the proto-solar nebula; essentially, a snapshot of the Solar System at its formation. For a full, detailed discussion, see McSween and Huss (2010).

Within these very primitive meteorites, there is a glue ("matrix") that holds the rock together. Very simply, this is a fine-grained dust which can contain large isotopic anomalies when compared with any known compositions anywhere in the Solar System. These grains are typically C-rich (e.g., SiC, graphite, or nanodiamonds) or O-rich (e.g., alumina, spinel, hibonite, or silicates) and are termed presolar or stardust (Nittler and Ciesla, 2016). These presolar grains are literally time capsules from long-extinguished stars; their elemental and isotopic compositions represent the unaltered fingerprints of the nucleosynthesis of the building blocks of the Solar System and ourselves.

Among these astrophysical time capsules, SiC is the best-studied of all presolar grains: thousands of individual

* Corresponding author.
E-mail address: fgyngard@gmail.com (F. Gyngard).
[1] Deceased on July 30, 2015.
[2] Present address: Planetary and Geoscience Division, Physical Research Laboratory, Ahmedabad, Gujarat 380009, India.

https://doi.org/10.1016/j.gca.2017.09.031
0016-7037/

grains have been measured for their C, N and Si isotopic compositions – see the Presolar Grain Database (Hynes and Gyngard, 2009) and references therein – and many of these grains have been measured for additional isotopic systems, as well. Primarily based on these C, N, and Si isotopic compositions, presolar SiC have been divided into different populations, termed Mainstream, AB, X, Y, Z, and nova (Hoppe et al., 1994; Hoppe and Ott, 1997). Mainstream grains are characterized by $^{12}C/^{13}C$ ratios between 10 and 100 and $\delta^{29}Si/^{28}Si$ and $\delta^{30}Si/^{28}Si$ values ranging from −50 to +200‰ (delta notation: $\delta^{i}X/^{j}X = [(^{i}X/^{j}X)_{measured}/(^{i}X/^{j}X)_{\odot} - 1] \times 1000$). Type AB grains have $^{12}C/^{13}C < 10$ and Si isotope compositions similar to mainstream grains. The rare type X grains are massively depleted in ^{29}Si and ^{30}Si relative to ^{28}Si (by 100 s of permil) and have $^{12}C/^{13}C$ ratios from 10 to 10,000. Type Y grains have $^{12}C/^{13}C > 100$ and $\delta^{29}Si/^{28}Si < \delta^{30}Si/^{28}Si$ compared to mainstream and type AB grains while type Z grains have mainstream-like $^{12}C/^{13}C$ ratios accompanied by values of $\delta^{29}Si/^{28}Si \ll \delta^{30}Si/^{28}Si$. An extremely rare number of SiC grains, with very low $^{12}C/^{13}C$ and $^{14}N/^{15}N$ ratios (<5 and <10, respectively) and large ^{30}Si excesses, have been classified as type "nova" grains, which is indicative of their speculative origin (see José and Hernanz, 2007). Apart from all of these, there is an additional extremely rare new class of SiC grains, type C, which have large ^{29}Si and ^{30}Si excesses (Croat et al., 2010; Hoppe et al., 2012). However, type X, C, and nova grains are not relevant to this paper and will not be discussed in further detail.

Comparison of the gross isotopic compositions of these different grain types to the compositions both measured in and predicted for various astrophysical settings has led to well accepted origin scenarios for each grain type – see Zinner (2007) for an overview. Mainstream, type Y, and type Z grains have been attributed to an origin in low-mass (1–5 $M_{\odot}$) AGB stars of approximately close-to-solar, half-solar, and one-third-solar metallicity, respectively. The origin of type AB grains is perhaps more enigmatic than that of the other SiC grain types, with two astrophysical sites – poorly understood J-type carbon stars and born-again AGB stars such as Sakurai's object – having been proposed for the grains' progenitors (Amari et al., 2001b).

Despite the wealth of available isotopic data for SiC, as well as the fact that Ti is one of the most abundant trace elements in SiC, only approximately 160 SiC grains have had their Ti isotopic composition determined (Amari et al., 2001a, 2001b; Ireland et al., 1991; Hoppe et al., 1994; Huss and Smith, 2007; Zinner et al., 2007). Of these previous studies, most Ti measurements (~100) have been disproportionately performed on the rare types AB, Y, X, and Z, which only constitute a combined 7% of the entire presolar SiC population. In addition, for the roughly 60 mainstream grains that have been analyzed for Ti, the data have not been obtained from a representative sample of the larger mainstream SiC population as a whole. Primarily due to earlier instrumental difficulties in measuring elements of low concentrations in small particles, the previous studies focused on either analyzing grains with large ^{29}Si and ^{30}Si excesses (Hoppe et al., 1994) or grains with high concentrations of Ti (Alexander and Nittler, 1999). The former criterion was chosen in order to ensure that there would be a greater chance that the grains would have significant Ti isotopic anomalies, while the latter analytical protocol was performed so as to achieve the best counting statistics possible. The study by Huss and Smith (2007) reported the Ti isotopic compositions of some large (4 – 9 μm in diameter) SiC from the Orgueil meteorite; due to their large sizes, these grains are not typical of the majority of presolar SiC grains.

Titanium in mainstream, type AB, and type Y SiC grains is usually characterized by enrichments in ^{46}Ti, ^{47}Ti, ^{49}Ti, and ^{50}Ti relative to ^{48}Ti, as evidenced by the V-shape isotopic pattern first observed by Ireland et al. (1991) and later by Hoppe et al. (1994) and Huss and Smith (2007). Enrichments in the secondary isotopes of Ti are in qualitative agreement with theoretical predictions for AGB stars, in which Ti isotopic compositions are affected by the slow capture of neutrons (*s*-process) in the He shell. Multiple dredge-up episodes, which occur after thermal pulses during the thermally pulsing asymptotic giant phase, periodically bring the products of He-burning and neutron capture nucleosynthesis into the H-rich convective envelope of the star, where the grains condense (Lugaro et al., 1999). This process will be discussed in more detail later. However, the Ti isotopic patterns observed for most of the grains measured by Alexander and Nittler (1999) fail to agree with theoretical predictions of a V-shaped pattern. Whether or not this discrepancy is due to some artifact of grain selection or to limited statistics is an unresolved problem requiring more extensive study.

The majority of the existing Ti isotopic data for presolar SiC grains have been shown to plot on linear correlation lines in Ti 3-isotope plots (Hoppe et al., 1994; Alexander and Nittler, 1999; Huss and Smith, 2007). This is similar to the situation for the Si isotopes, which show correlated excesses of ^{29}Si and ^{30}Si relative to ^{28}Si, indicative of a combination of a strong galactic chemical evolution (GCE) component (Zinner et al., 2006) and isotopic heterogeneity in the local interstellar medium (ISM) affecting the Si isotopes (Lugaro et al., 1999). Likewise, for Ti, the observed correlated spread in Ti isotopic ratios indicates that GCE must be largely responsible for the Ti compositions in the grains, and this is further evidenced by the linear correlation seen between Ti isotopic ratios and the corresponding $\delta^{29}Si/^{28}Si$ values. However, the GCE of the Ti isotopes is still not well understood, and models of isotopic heterogeneity in the ISM fail to reproduce the Si-Ti isotopic correlations (Nittler, 2005).

In order to eliminate as much sample bias as possible and expand the existing dataset of grains analyzed for Ti, we have attempted to measure the Si and Ti (along with the C and N) isotopic ratios in a large number (~250) of presolar SiC grains with a nanoscale secondary ion mass spectrometer (SIMS), the NanoSIMS. This instrument affords us the ability to make high-mass-resolution measurements at higher transmission than was available for the previous Ti analyses (which employed either Cameca IMS 6f or SHRIMP 1 ionprobes), allowing for more precise determination of this low abundance element. The grains analyzed in this work are from the KJG SiC-rich fraction

(Amari et al., 1994) of the Murchison meteorite and were not preferentially selected, with the only caveat being that well-separated grains of diameter ~2.5 μm and greater were chosen. This lower limit on grain size was put in place only to ensure the best chance of measuring the isotopic compositions of multiple elements (C, N, and Si), while still leaving enough grain material for sufficiently precise Ti measurements. Here we report the C, N, Si, and Ti isotopic compositions of 220 mainstream, 10 type AB, 4 type Y, and 4 type Z presolar SiC grains (expanding the total number of SiC grains analyzed for Ti roughly two-fold), and compare these compositions to the existing dataset. In addition, since the mechanism for the chemical incorporation of Ti into presolar SiC grains is currently uncertain, the data presented here can provide new information to help determine whether Ti resides in the grains as subgrains or in solid solution. Preliminary reports of some of the data and conclusions of this work have been presented previously in two conference abstracts (Gyngard et al., 2006a, 2006b).

2. EXPERIMENTAL DETAILS

A detailed description of the chemical separation procedure developed for the isolation of SiC grains from the Murchison (CM) meteorite has been given by Amari et al. (1994). Briefly, this process principally consisted of progressively applying corrosive solvents to remove various mineral phases one by one, typically dissolving silicate material in hydrofluoric acid and the remaining chromite (Cr_2O_3) and carbonaceous organic matter in perchloric acid. The subsequent aliquots were then separated by size by centrifugation into several fractions, enriched in SiC grains to ~70%. Samples of the resulting SiC-rich residue studied here, KJG, with typical grain diameters ranging from 2 to 4.5 μm, were then deposited from liquid suspension onto high purity Au foil and manually scanned for well-separated grains with a JEOL 840A SEM. After confirmation as SiC by energy dispersive X-ray (EDX) analysis, 247 grains of diameter roughly greater than 2.5 μm were randomly selected for isotopic measurements in the Washington University NanoSIMS. Under bombardment of a Cs^+ primary beam of a ~1 pA and ~100 nm in diameter, negative ion signals of ^{12}C, ^{13}C, ^{28}Si, ^{29}Si, and ^{30}Si were produced from the grains and simultaneously counted with five electron multipliers (EMs) in multi-detection mode. Subsequently, the N isotopic ratios were determined from parallel detection of the $^{12}C^{14}N^-$ and $^{12}C^{15}N^-$ signals in a separate analysis session. A powdered sample of synthetic SiC was used for normalization of the C and Si isotopic ratios, while a fine grained mixture of SiC and Si_3N_4 was used for calibration of the N isotopic ratios. The absolute isotopic compositions of these materials are not known; however, they are all synthetic and the assumption of approximately solar composition is valid. For the purposes of identification and classification of presolar grains having large isotopic anomalies, these standards are sufficient. The $^{14}N/^{15}N$ ratio of the SiN standard is consistent within statistical uncertainties of terrestrial air (272).

The Ti isotopic compositions of 238 of the grains – nine grains of the original 247 measured for C, N, and Si could not be relocated for Ti analysis and were likely sputtered away by the previous analyses – were determined in the NanoSIMS in combined mode, which is a combination of magnetic peak jumping and multi-detection. Positive secondary ions of Ti were produced by bombardment of the grains with an O^- primary beam ~500–1000 nm in diameter (smaller than the average grain diameter in order to eliminate contamination from surrounding material), with an intensity of several 10s of pA. Three magnetic field settings were needed in order to measure all the isotopes of Ti, as well as to monitor signals from ^{44}Ca (to correct for isobaric interferences of Ca at masses 46 and 48) and ^{51}V and ^{52}Cr (to correct for isobaric interferences of V and Cr at mass 50). In the first field step, we measured ^{28}Si, ^{44}Ca, ^{46}Ti, and ^{48}Ti with EMs 1 through 4; ^{46}Ti, ^{48}Ti, ^{50}Ti, and ^{52}Cr were monitored in the second field step with detectors 2 through 5; and in the final step, ^{47}Ti, ^{49}Ti, ^{51}V, and ^{53}Cr were also detected with EMs 2 through 5. By assuming solar isotopic ratios of Ca, V, and Cr, the corrected $^{50}Ti/^{48}Ti$ isotopic ratio, for example, can be expressed as:

$$\frac{^{50}Ti}{^{48}Ti} = \frac{\left(\frac{S_{50}}{S_{48}}\right)_{measured} - \left(\frac{^{50}Cr}{^{52}Cr}\right)_{solar} \times \left(\frac{^{52}Cr}{S_{48}}\right)_{measured} - \left(\frac{^{50}V}{^{51}V}\right)_{solar} \times \left(\frac{^{51}V}{S_{48}}\right)_{measured}}{1 - \left(\frac{^{48}Ca}{^{44}Ca}\right)_{solar} \times \left(\frac{^{44}Ca}{S_{48}}\right)_{measured}} \quad (1)$$

where S_{48} and S_{50} represent the total measured signals with all isobaric interferences included at masses 48 and 50, respectively. In a similar manner, the $^{46}Ti/^{48}Ti$ isotopic ratio can be corrected for ^{46}Ca. The magnitude of these corrections is small, almost invariably less than a few permil for Ca and approximately 5–10‰ for V. The correction for ^{50}Cr on ^{50}Ti was usually less than 10‰, although in some cases (particularly for grains with large Cr subgrains) the contribution could be up to a few 100‰; however, the large observed Cr contents are most likely artifacts from the chemical separation procedure, which included treatment with dichromate ($Cr_2O_7^=$). Due to our experimental setup, we were able to determine $^{53}Cr/^{52}Cr$ ratios, all of which are isotopically normal both whether in subgrains or not. Even in situations where the Cr interference corrections are substantial, the assumption of solar isotopic ratios is reasonable; AGB stars do not produce large (>10‰) isotopic anomalies in Cr isotopes.

Elemental abundance estimates of Ti and V depend critically on relative sensitivity factors (RSF). An RSF of 3.82 for Ti relative to Si had been previously determined in our lab from measurements on a NIST SRM 610 silicate glass standard; however, this value was quite variable (several percent) over multiple measurement sessions. The Ti RSF from the literature has also been shown to be quite variable, ranging from a value of 4.2 (Besmehn and Hoppe, 2003) up to 4.57 (Hinton, 1990) calculated for an updated SRM 610 Ti concentration of 460 (Rocholl et al., 1997). Sensitivity factors can often be strongly affected by instrumental tuning conditions and sample morphology and height, particularly for the NanoSIMS, as the ion extraction optics are much closer to the sample surface than in conventional ion-probes. To encompass this overall uncertainty in the RSF from multiple authors, we decided to take an average of these reported RSF values and our own, yielding a value of 4.19. Huss and Smith (2007) reported a useful yield of Ti relative to Si of ~10 times for Ti in Si under O^- beam

primary bombardment with a Cameca IMS 6f instrument. As they did not standardize their measurements, no absolute RSF can be determined from their work; thus, we prefer to use the average value calculated from ours and the other previous studies as it is more typical of RSFs determined for NanoSIMS instruments. A V to Si sensitivity factor of 3.83 was determined by averaging an RSF of 3.76 measured in our lab with a re-evaluated Hinton (1990) value of 3.89. No other NanoSIMS studies have reported V RSFs. Due to the fact that the ionization efficiency of Si and other elements in a glass, such as NIST 610, is different than that for a SiC matrix, we cannot report absolute elemental abundances, only relative ones. We do not have synthetic SiC grains doped with known trace elemental concentrations for a one-to-one comparison. It should also be noted that, unfortunately, during the measurement of 75 grains, the ^{51}V mass-peak was lost, and therefore no V concentrations can be reported for them. The most likely explanation for the loss of this peak is that for both the grains and the standards, V concentrations were extremely low. Thus, any small mass shift off of the peak can be hard to detect – as only one isotope of V was able to be directly measured, V isotopic ratios could not be used to confirm the peak was centered, even for the standards. Regardless, as the correction for ^{50}V on ^{50}Ti is very minor (only a few permil for the other grains in which ^{51}V was successfully monitored), this oversight should not significantly affect our results for ^{50}Ti in grains not measured for V.

3. RESULTS

3.1. C, N, and Si isotope data

The C, N, and Si ratios of the grains measured for Ti are given in Supplemental Table 1 and plotted in Fig. 1a. Among the 238 grains analyzed for their Ti isotopic compositions, we identified 10 type AB grains (4.2% by number), 4 type Y grains (1.7%), 4 type Z grains (1.7%), and 220 mainstream grains (92.4%) (Fig. 1a and b) based on their C, N and Si isotopic compositions, which is roughly within the range of grain type abundances seen previously (Hoppe and Ott, 1997). We have characterized grain 1m2-1 as type Y, based on its Si isotopic composition, with an excess in ^{30}Si relative to the mainstream line, although its ^{12}C/^{13}C ratio of 72.7 does not agree with the standard classification for type Y grains, which are defined to have ^{12}C/^{13}C > 100. One grain (61-1) with a ^{12}C/^{13}C ratio greater than 100 has been classified as type Z, in contrast to the ^{12}C/^{13}C ratios for most Z grains, because its Si isotopic composition is more consistent with that of type Z grains. The average ^{12}C/^{13}C ratio of the 238 grains is 56.1, in good agreement with the value of ~56 seen in previous results by Nittler and Alexander (2003) for a very large population (a few 1000s) of grains.

The Si isotopic ratios, expressed as δ-values, are shown in a Si three-isotope plot in Fig. 1b and presented in Supplemental Table 1. For clarity, the errors are not plotted, but are largely dominated by the standard deviation of measurements on standards and are typically less than 4‰ for δ^{29}Si/^{28}Si and less than 6‰ for δ^{30}Si/^{28}Si, yielding some

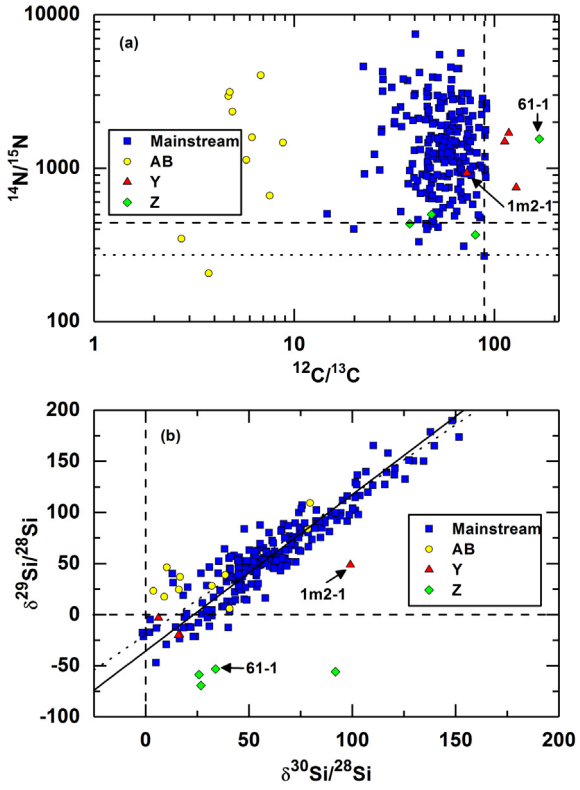

Fig. 1. Carbon, N, and Si isotopic ratios of the 238 SiC grains analyzed for their Ti isotopic compositions. The dashed lines in this figure, and all subsequent ones, represent solar isotopic ratios. Grains 61-1 and 1m2-1 have been classified as type Z and Y grains, respectively, based solely on their Si isotopic composition. (a) Plot of the grains' C and N isotopic ratios. The dotted line represents the terrestrial N isotopic ratio which was used to normalize the data; this has been done to maintain historical consistency with previous N results for presolar SiC. (b) Three-isotope plot of the grains' Si isotopic compositions, expressed as δ-values, or deviations from solar isotopic ratios in parts per thousand (‰). The dotted line represents the SiC mainstream correlation line of δ^{29}Si/^{28}Si = −19.9 + 1.37 × δ^{30}Si/^{28}Si (Zinner et al., 2007); the solid line is the result of a weighted least-squares fit to the Si isotopic composition of the mainstream grains analyzed in this study, corresponding to δ^{29}Si/^{28}Si = −35.6 + 1.53 × δ^{30}Si/^{28}Si.

of the most precise Si isotopic measurements on presolar SiC to date. Although to first order the data are similar to previous measurements on presolar SiC, at least two notable differences can be observed. First, there are no grains with δ^{30}Si < 0, within statistical uncertainties. In addition, based on an expected ~1% abundance of type X grains, we would expect 2 X grains in this study; however, finding a null return is within statistical fluctuations. Second, an error-weighted least-squares fit – with δ^{30}Si/^{28}Si as the abscissa and δ^{29}Si/^{28}Si as the ordinate – to the 220 mainstream grains presented here yields a line of slope 1.53 ± 0.02 and an intercept of −35.61 ± 1.53, in contrast with the "mainstream correlation line" of slope 1.37 ± 0.01 and intercept −19.9 ± 0.6, derived from previous measurements of several thousand mainstream presolar SiC grains (Zinner et al., 2007). A detailed comparison of

the Si (and Ti) isotopic compositions of the KJG grains analyzed here with previous measurements of presolar SiC is discussed in the following section, particularly in the context of the deviation in Si isotopes from the majority of grains in the literature, as well as with prior measurements of Ti isotopes in mainstream SiC. In Table 1, a comprehensive list of the slopes, intercepts, and reduced chi-squared values is given for all the error-weighted least-squares fits (with errors) for the relevant correlation lines reported throughout this work. Also compared are the Si correlation lines corresponding to the new data with that of previous KJG data, which show a shallower slope.

3.2. Ti isotope data

The Ti isotopic compositions of the 238 grains of this study are given in Supplemental Table 1 and displayed in Fig. 2 and are seen to correlate well with $\delta^{29}Si/^{28}Si$ values (Fig. 3). As has been observed in other analyses of Ti isotopes in mainstream SiC (Hoppe et al., 1994; Alexander and Nittler, 1999; Huss and Smith, 2007), the Ti isotopic data exhibit strong linear correlations, though less so for ^{50}Ti (Fig. 2a), which is a magic number nucleus. For nuclei to be "magic," the number of protons or neutrons (or both for "double magic") must completely fill a set of nuclear shells, resulting in particularly tightly bound nuclei with small n-capture cross-sections. For nucleosynthesis in AGB stars, large overabundances of magic number nuclei are expected as they are significantly less affected by n-capture than other isotopes of a given element, owing to their smaller cross-sections.

The range of $\delta^{46}Ti/^{48}Ti$, $\delta^{47}Ti/^{48}Ti$, $\delta^{49}Ti/^{48}Ti$, and $\delta^{50}Ti/^{48}Ti$ values is generally consistent with previous results; however, similar to the Si isotopes, some differences (such as elevated $\delta^{50}Ti/^{48}Ti$ values, for example) between the Ti compositions measured here and the previous results for mainstream SiC are apparent. This will be discussed further below.

3.3. Vanadium-51 Data

As can be seen in Supplemental Table 1 and Fig. 5, V concentrations in the grains are, in general, approximately a factor of 10 smaller than those of Ti, roughly consistent with the solar system elemental V/Ti ratio of 0.12 (Lodders, 2003) derived from CI chondrites and the solar photosphere. The elemental abundances of both Ti and V can be seen to be fairly well correlated (Fig. 5), which is expected, as Ti and V are both refractory and chemically similar. Good elemental correlation between Ti and V has

Table 1
Error-weighted least-squares fits to the populations of mainstream presolar SiC grains discussed in the text.

X vs Y	Fit[a]	This work	HAH[b]	Combined[c]	Other KJG[d]	GCE[e]
$\delta^{30}Si/^{28}Si$ vs $\delta^{29}Si/^{28}Si$	m	1.53 ± 0.02	1.52 ± 0.04	1.52 ± 0.02	1.43 ± 0.03	0.96
	b	-35.61 ± 1.53	-29.57 ± 2.26	-33.77 ± 1.24	-25.95 ± 2.00	0
	χ^2	2.76	2.06	2.66	2.01	
$\delta^{46}Ti/^{48}Ti$ vs $\delta^{47}Ti/^{48}Ti$	m	0.51 ± 0.02	0.52 ± 0.03	0.52 ± 0.02		0.92
	b	-15.36 ± 0.91	-8.95 ± 2.35	-14.51 ± 0.86		0
	χ^2	0.79	0.61	0.80		
$\delta^{46}Ti/^{48}Ti$ vs $\delta^{49}Ti/^{48}Ti$	m	0.78 ± 0.03	0.92 ± 0.05	0.85 ± 0.02		0.53
	b	67.06 ± 1.13	27.41 ± 3.27	59.61 ± 1.13		0
	χ^2	3.49	3.43	4.27		
$\delta^{46}Ti/^{48}Ti$ vs $\delta^{50}Ti/^{48}Ti$	m	2.41 ± 0.08	1.73 ± 0.08	2.59 ± 0.08		1.13
	b	122.0 ± 2.86	47.44 ± 5.40	101.8 ± 3.11		0
	χ^2	9.79	4.23	10.26		
$\delta^{29}Si/^{28}Si$ vs $\delta^{46}Ti/^{48}Ti$	m	0.86 ± 0.02	1.16 ± 0.05	0.90 ± 0.02		1.14
	b	-16.38 ± 1.34	-14.40 ± 2.92	-16.20 ± 1.21		0
	χ^2	4.03	3.94	4.34		
$\delta^{29}Si/^{28}Si$ vs $\delta^{47}Ti/^{48}Ti$	m	0.44 ± 0.02	0.57 ± 0.04	0.45 ± 0.02		1.05
	b	-25.66 ± 1.18	-15.37 ± 2.27	-23.45 ± 1.04		0
	χ^2	1.99	2.36	2.52		
$\delta^{29}Si/^{28}Si$ vs $\delta^{49}Ti/^{48}Ti$	m	0.67 ± 0.02	0.99 ± 0.04	0.74 ± 0.74		0.61
	b	54.27 ± 1.32	16.12 ± 2.48	46.44 ± 1.18		0
	χ^2	4.41	6.24	5.52		

Notes. The mainstream correlation line is given by $\delta^{29}Si/^{28}Si = (-19.9 \pm 0.6) + (1.37 \pm 0.01) \times \delta^{30}Si/^{28}Si$ (Zinner et al., 2007).

[a] Parameters for a linear regression with m, b, and, χ^2 corresponding to the slope, intercept, and reduced χ^2, respectively; errors are determined by including uncertainty in the fits due to the one sigma experimental errors.

[b] Data from grains measured for Ti from Hoppe et al. (1994), Alexander and Nittler (1999), and Huss and Smith (2007).

[c] Combination of the isotopic data of this study and that of HAH (column 4).

[d] KJG grains previously measured for Si isotopes from the same size fraction as those of this work. No Ti results are available for these grains.

[e] Normalized GCE predictions from Timmes et al. (1995) – also see Alexander and Nittler (1999).

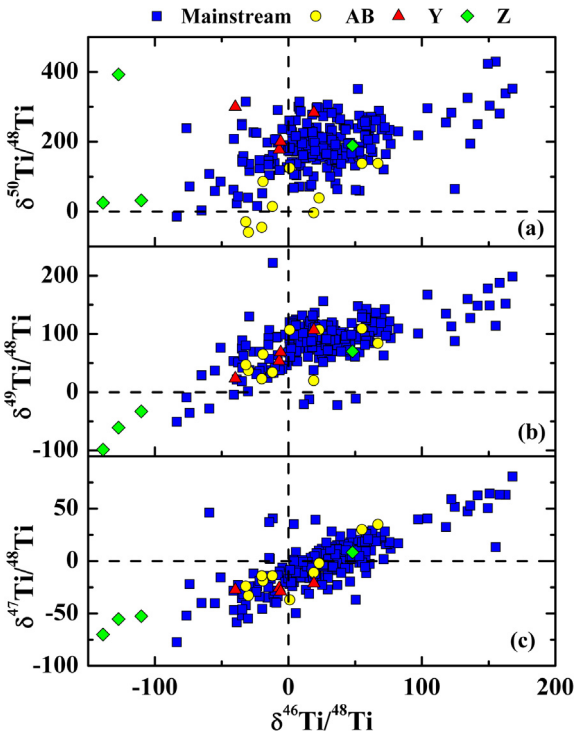

Fig. 2. Titanium isotopic ratios of the SiC grains measured in this study, expressed as δ-values, with $\delta^{47}Ti/^{48}Ti$, $\delta^{49}Ti/^{48}Ti$, and $\delta^{50}Ti/^{48}Ti$ plotted against $\delta^{46}Ti/^{48}Ti$.

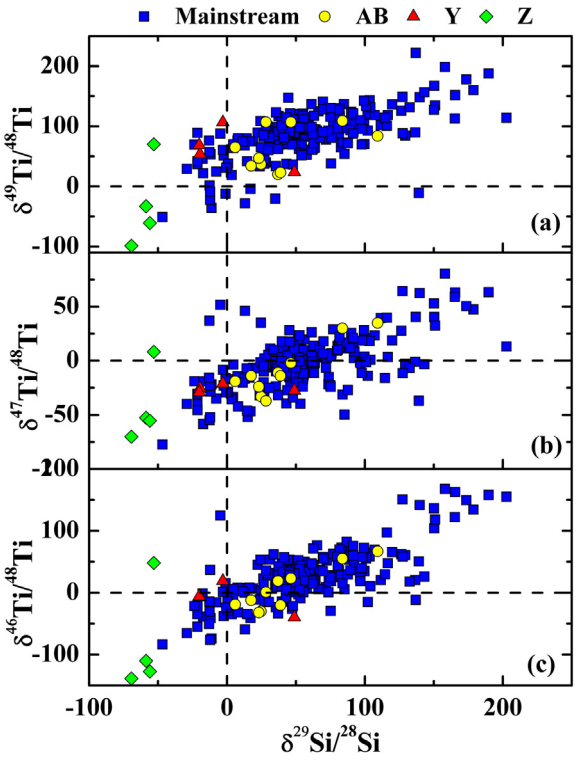

Fig. 3. Plot of $\delta^{46}Ti/^{48}Ti$, $\delta^{47}Ti/^{48}Ti$, and $\delta^{49}Ti/^{48}Ti$ values against $\delta^{29}Si/^{28}Si$ values. As mentioned in the text, ^{50}Ti is a particularly stable nucleus, thus $\delta^{50}Ti/^{48}Ti$ values do not correlate well with Si isotopes and are not shown.

been seen before in measurements of K-series SiC grains (Amari et al., 1995). Out of the 136 grains measured for both Ti and ^{51}V and which also showed evidence for Ti-rich subgrains, of which 27 grains showed no evidence, the ^{51}V signal correlates well with the Ti signal in 132 of the grains (97%), e.g., Fig. 4, as the grains are being sputtered away.

4. DISCUSSION

4.1. Ti contents: solid solution of TiC subgrains?

Transmission electron microscope (TEM) analyses of SiC ultra-microtome sections (Bernatowicz et al., 1992; Stroud and Bernatowicz, 2005) show the presence of many internal TiC crystals, from roughly 10 to 100 nm in diameter. TEM observations that the TiC subgrains have an epitaxial relationship with the SiC matrix supports the idea of a formational relationship between the TiC subgrains and the surrounding SiC grain. In situ formation is opposed to the possibility of TiC forming first as free-floating crystals to be later encapsulated by condensing SiC, as is often the case for presolar graphite, in which TiC can serve as the nucleation center for the grain (Croat et al., 2003) and where no orientational relationship between subgrain and host grain exists. Despite Ti being an abundant trace element in presolar SiC and having been observed in several TEM studies, it remains an open question whether the Ti in the *majority* of presolar SiC grains resides in the grains as distinct subgrains or in solid solution within the SiC crystal lattice. Based on Ti measurements from the large number of grains of this study, we will demonstrate that, whether or not Ti was initially incorporated as solid solution during grain condensation, by the time the grains

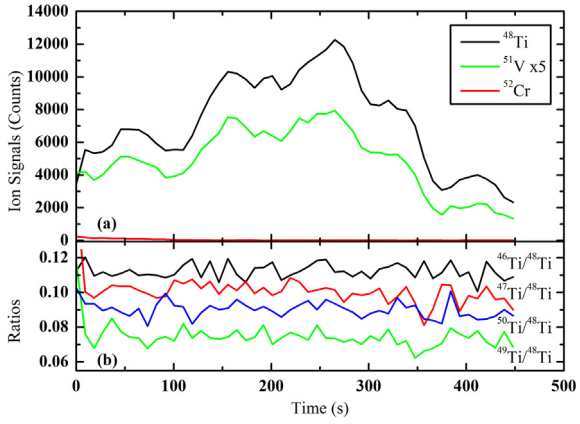

Fig. 4. Depth profiles of Ti, V, and Cr signals and corresponding Ti isotopic ratios for presolar SiC grain 1m2-1. (a) Plot of the ^{48}Ti, ^{51}V (multiplied by a factor of 5), and ^{52}Cr signals as a function of depth (i.e., measurement time) as the primary beam sputters through the grain: Ti and V are correlated, showing large variability due to the presence of subgrains, similar to what is seen for at least 80% of the grains analyzed. (b) Plot of the Ti isotopic ratios of grain 1m2-1 as a function of depth, displaying little isotopic heterogeneity throughout the grain. The variations shown are due to counting statistical fluctuations.

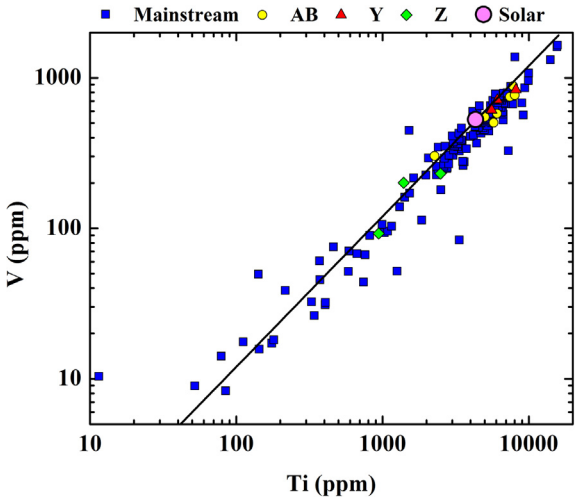

Fig. 5. Plot of the Ti and V abundances for the grains analyzed for both Ti and V. The black line is an error-weighted best-fit to the data. See text for details.

entered the low temperatures of interstellar space, for the majority of SiC grains the Ti in must have been present as subgrains. Of the 238 grains analyzed for Ti in this study, at least 80% show large fluctuations in Ti concentrations (Fig. 4a) as the grains are sputtered away during NanoSIMS analysis, indicative of the presence of Ti-rich subgrains. While it is tempting to try to estimate the size of the subgrains by inferring the NanoSIMS sputter rate and calculating the expected Ti signal for a grain of a given size, this is not realistic. As these measurements were not performed in isotope imaging mode, no spatial information can be gleaned from the data; for instance, the variability in the Ti ion signal could either be from one large subgrain or from a cluster of smaller grains distributed heterogeneously. As each measurement cycle is a gross average of the entire grain, we cannot distinguish between either case. Previous studies (e.g. Huss and Smith, 2007) have also observed large variability in the Ti/Si ratios in presolar SiC, as a function of depth in the grain. Although isotopic measurements alone cannot unequivocally determine whether these observations actually are definitive proof of crystalline subgrains, the non-uniformity of Ti concentrations throughout individual grains argues against the idea that Ti is present in solid solution, in which Ti is substituted for Si in the SiC crystal lattice. It is possible, though unlikely, that Ti could still be in solid solution, but *heterogeneously* distributed (where Ti could have substituted for Si only in isolated areas of the overall crystal structure), in principle mimicking the Ti variability seen in the isotopic signals. However, further evidence that Ti is present as TiC subgrains, and not in solid solution, in presolar SiC is given by the presence of V in the grains. Titanium and V are chemically very alike (both are similarly refractory elements) and this observed correlation between Ti and V should not be surprising as $Ti^{4+}C$ and $V^{4+}C$ form isostructural crystals, with C at interstitial sites, allowing for V to substitute for Ti in TiC. If Ti were present only in solid solution, there is no reason a priori for the V signal to trace with the Ti signal. NanoSIMS observations of correlated Ti and V signals are qualitatively consistent with TEM-EDX measurements of TiC subgrains in presolar graphite, which almost invariably contain V, often with V/Ti ratios elevated relative to solar values (Croat et al., 2003).

For reasonable estimates of photospheric temperatures in AGB stars, equilibrium thermodynamics calculations show that TiC initially condenses at temperatures from 1565 to 1805 K, whereas SiC forms between 1390 and 1630 K (Lodders and Fegley, 1995; Bernatowicz et al., 1996). Since the condensation temperature of SiC is significantly lower than that of TiC, TiC subgrains are expected to form first and to be incorporated as distinct crystals in the SiC matrix, like TiC into presolar graphite; however, though limited, the TEM observations mentioned above of TiC subgrains in SiC are not compatible with this scenario. A formational association in which TiC and SiC could nucleate simultaneously may be obtained if the grains condensed from a supercooled gas. Alternatively, as proposed by Bernatowicz et al. (1996), Ti may have been present initially in solid solution, but later exsolved into distinct crystals due to long exposure to high temperatures in the stellar atmosphere. Either way, once the SiC grains were ejected into the cold interstellar space, significant modification of their crystal structure is unlikely to have occurred. The observations of variations in Ti and V presented here cannot distinguish between these possibilities and only by more TEM observations of TiC in SiC can the issue be absolutely settled; however, the high percentage of grains with evidence for Ti-rich subgrains (as well as correlated V contents, see Fig. 4a) in the present study leads to the conclusion that the majority of *all* presolar SiC possess Ti-rich subgrains. In fact, the high percentage of SiC grains containing Ti-rich subgrains given above is only a lower limit, as in some cases (in particular for grains with low Ti concentrations) it can be difficult to determine whether small fluctuations in Ti signals are in fact from tiny subgrains or simply a statistical effect due to low count rates. Unfortunately, to avoid prohibitively long data acquisition times, the analyses were not performed in isotopic imaging mode and we cannot determine the size or distribution of the subgrains. It is possible, for example, that what may appear as a large, singular spike in the Ti signal may be actually from a pocket or clump of small subgrains. It is challenging to absolutely state that the Ti isotopic anomalies are entirely carried by the subgrains, as most grains contain subgrains which dominate the overall Ti contents of the grains. Nonetheless, in general, it does not appear that the subgrains within an individual grain have any appreciable isotopic differences from each other (Fig. 4b), within statistical uncertainties, leading to the conclusion that the gas in the stellar envelope where and when the host SiC grain condensed must have been relatively homogeneous in Ti isotopic composition, at least in the order of a few tens ‰. As will be discussed later, this is not entirely unexpected, as the Ti isotopes of the grains are largely dominated by GCE signatures and only modest shifts of most Ti isotopic ratios are expected from nucleosynthesis in low-mass AGB stars of solar metallicity; hence, large Ti isotopic heterogeneity is unlikely. In addition, one wouldn't expect

any changes in the isotopic ratios in the envelope of an AGB star during grain condensation, as grains likely condense on a time scale of years. However, changes in the envelope compositions are expected to come from third dredge-up after thermal pulses, with each pulse separated by thousands of years.

Approximately 30% of the grains also show evidence for Cr subgrains, as evident by large increases in the ^{52}Cr signal, which only rarely correlates with either Ti or V. It is unlikely these represent indigenous subgrains, as Cr_2O_3 was applied to the residue during the grain separation process in order to remove reactant kerogens (Amari et al., 1994), and may have diffused through the (often) etched grain surfaces. The fact that all the grains' $^{53}Cr/^{52}Cr$ ratios, whether in subgrains or not, were normal supports this; however, large Cr isotopic anomalies are not expected to be produced by AGB stars. Additionally, as Cr is relatively less volatile than Ti and Si, it is not predicted to condense into SiC grains, as minerals such as Cr3C2 are expected to form at lower temperatures than TiC and SiC (Ebel, 2006).

Titanium concentrations from grain to grain vary by over two orders of magnitude, from ~40 ppm to over 15,000 ppm, with a significant number of grains at both ends of this Ti abundance range (Fig. 6). Such marked variation in abundances from grain to grain may reflect fundamental differences in temperature and pressure for the region of the gaseous envelope where the grains condensed. As the condensation temperature for TiC is higher than that of SiC, if a SiC grain begins to condense in a cooler (and lower pressure) environment, the amount of Ti available to be incorporated into the grain will be depleted compared to SiC condensing at higher temperatures, leading to correspondingly lower absolute abundances. The observed spread in Ti elemental abundances may also simply be a temporal effect: grains that condense later in the thermally pulsing phase may have significantly less Ti available for incorporation, as successive TDU episodes do not bring more Ti contents up from the He-burning shell into the envelope where the SiC form; therefore, grains that begin their condensation after fewer TDU episodes will have, in general, higher *s*-process heavy (trace) element abundances.

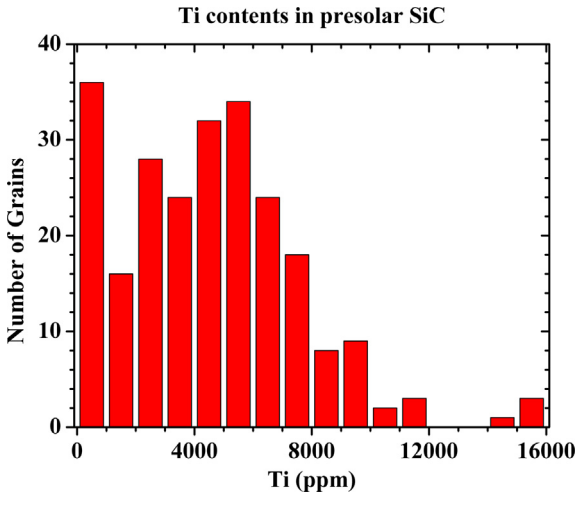

Fig. 6. Histogram showing the distribution of Ti contents (ppm by weight) for the sample of grains analyzed in this study. Ti concentrations from grain to grain vary by up to 2 orders of magnitude. About 10% of the grains have Ti abundances less than 500 ppm.

The Ti abundances are well within previously observed values, although concentration values for individual grains are often not explicitly given in the literature. However, it does seem that the abundances determined in the present study are somewhat higher than those determined for SiC from the LS + LU fractions (Virag et al., 1992), the KJH fraction (Hoppe et al., 1994), Amari et al. (1995) as determined by energy filtering analysis, and from the Orgueil meteorite (Huss and Smith, 2007). These fractions all have average grain sizes larger than the KJG grains analyzed in this work – LS + LU SiC have nominal grain diameters of 5 μm and greater, KJH SiC have an average grain diameter of ~4.6 μm, and the Orgueil grains measured for Ti were all chosen to be greater than ~4 μm. The observation of higher Ti concentrations in KJG SiC (average grain diameter ~3 μm) is consistent with previous observations showing that trace element abundances increase as grain size decreases (Virag et al., 1992; Amari et al., 1995). It is also worth remarking here that there do not appear to be any obvious correlations among Ti concentrations, the presence of subgrains, or the Ti isotopic compositions of the grains; one might expect that the grains without subgrains may have generally lower Ti abundances, but apparently this is not the case.

4.2. Comparisons with Previous Si Isotopic Data

As mentioned above, the Si isotopic compositions of the grains measured here differ somewhat from previously reported SiC grain data. Discrepancies between our measurements and the larger preexisting datasets may be due to the fact that not manySiC grains of this size fraction have previously been measured for their Si isotopic ratios – only 154 other analyses of mainstream KJG grains have been reported. Most prior measurements of Si isotopes in SiC have been performed on either smaller grains, with a mean diameter of ~1 μm (Hoppe et al., 1996; Nittler and Alexander, 2003), or on larger grains, greater than 4 μm (Hoppe et al., 1994), than those measured here. In a random sampling of over 200 SiC grains, one would statistically expect to see at least a few grains with $\delta^{30}Si < 0$, though we did not find any grains with depletions in ^{30}Si in this study. Among the 154 previously analyzed mainstream KJG grains, there are 9, although only 4 are outside 1σ errors. However, it could simply be that we measured a unique population of grains, and the fact that our mainstream line is somewhat steeper and of lower intercept is a consequence of this selection. Although previous studies found little evidence for systematic deviations in Si isotopic composition as a function of grain size (Hoppe et al., 1996; Amari et al., 2000), our level of precision may allow us to constrain our data to an extent that subtle differences are observable. In addition, an error-weighted least-square fit to the Si isotopic data of the other KJG SiC grains that

have previously been analyzed yields a correlation line of $\delta^{29}Si/^{28}Si = -25.95\ (\pm 2.00) + 1.43\ (\pm 0.03) \times \delta^{30}Si/^{28}Si$ – see Table 1. This fit is in between the steeper slope (1.53) and lower intercept (−36) determined from the grains of this study and the best-fit slope of 1.37 and intercept of −20 of Zinner et al. (2007) derived from a larger data set of ~4100 grains, encompassing virtually all mainstream SiC grains analyzed which have reasonably small uncertainties. A possible, though speculative, explanation for the apparent difference between the mainstream correlation lines for KJG grains and the fit for the entire SiC population may lie in the fact that type Y and Z grains are more abundant among small SiC grains. For instance, it has been previously observed that for very small (0.25 – 0.65 μm) presolar SiC from the Indarch meteorite, the abundances of type Y and Z grains can be up to 6% and 8%, respectively (Zinner et al., 2007), as opposed to the 1% observed in size separates of greater than 1 μm. Because the mainstream correlation line of Zinner et al. (2007) is largely derived from measurements of grains 1 μm and smaller and because no exact standard definition exists for classification into different SiC grain types (which is therefore inherently subjective), some number of *marginal* type Y and Z grains may have been categorized as mainstream. Since these grain types have typical compositions of $\delta^{29}Si/^{28}Si < \delta^{30}Si/^{28}Si$, if a portion of them contributed to the mainstream correlation line, a best-fit line would have a lower slope and higher intercept than if they were not included, although it may be difficult to precisely determine the absolute magnitude of the effect. For the case of grains from the KJG fraction, in which type Y and Z grains are particularly rare, this dilution effect would be considerably less, thereby perhaps explaining the perceived difference in the correlation lines. It should also be noted here that the error-weighted least-square fit to the Si isotopic composition of the ~60 previous mainstream SiC for which Ti isotopic ratios have also been determined (Hoppe et al., 1994; Alexander and Nittler, 1999; Huss and Smith, 2007) is $\delta^{29}Si/^{28}Si = -29.6 + 1.52 \times \delta^{30}Si/^{28}Si$, in good agreement with the fit to the grains measured in this study. Interestingly, 8 of 10 AB grains plot to the left of the mainstream correlation line along a line with an intercept close to solar. This is to be expected if these grains originated from stellar sources which have not had significant *s*-process enhancements (Amari et al., 2001b). It remains to be seen whether high-precision Si isotopic measurements on many more AB grains will confirm this observation.

4.3. Comparisons with previous Ti isotopic data

As mentioned before, the $\delta^{46}Ti/^{48}Ti$, $\delta^{47}Ti/^{48}Ti$, $\delta^{49}Ti/^{48}Ti$, and $\delta^{50}Ti/^{48}Ti$ values measured in this study are comparable to previous analyses of Ti isotopes in presolar SiC grains. As pointed out above, in addition to mainstream grains, the Ti compositions of grains of types AB, X, Y, and Z have been specifically studied in several extensive, focused surveys. Type AB grains have been shown to have Ti isotopic compositions similar to those of mainstream grains (Amari et al., 2001b), and the compositions of the ten AB grains measured here are consistent with this prior result. Likewise, the four type Y grains measured here and those analyzed previously (Amari et al., 2001a) also do not, in general, have Ti isotopic compositions markedly different from those of mainstream grains, although a few grains from Amari et al. (2001a) do have significantly larger $^{49}Ti/^{48}Ti$ and $^{50}Ti/^{48}Ti$ ratios than most mainstream grains, suggestive of an origin in lower-than-solar metallicity stars. In contrast to types AB, Y, and mainstream grains, type Z grains are typically depleted in ^{46}Ti, ^{47}Ti, and ^{49}Ti and substantially enriched in ^{50}Ti, relative to ^{48}Ti (Zinner et al., 2007), generally consistent with the analyses here of four type Z grains. This overall Ti isotopic signature is consistent with the Si isotopic composition of type Z grains, with depletions in ^{29}Si and large ^{30}Si enhancements relative to ^{28}Si, indicative that ^{29}Si, ^{46}Ti, ^{47}Ti, and ^{49}Ti are primarily affected by GCE, whereas ^{30}Si and ^{50}Ti are more susceptible to n-capture in the parent stars of the grains. No grains of type X were discovered, and combined with the fact that these grains have a different astrophysical origin (SNe as opposed to AGB stars), their compositions will not be discussed.

The analyses presented here did not principally target rare grain types, and as such, we will focus the remaining discussion primarily on comparisons between the Ti isotopic compositions of mainstream grains analyzed here and those from the three largest previously reported datasets (Hoppe et al., 1994; Alexander and Nittler, 1999; Huss and Smith, 2007), which will be referred to as HAH. Displayed in Fig. 7 are the Ti isotopic data for mainstream SiC grains from HAH and this work, and, in Fig. 8, the $\delta^{46}Ti/^{48}Ti$, $\delta^{47}Ti/^{48}Ti$, and $\delta^{49}Ti/^{48}Ti$ values are shown along with the $\delta^{29}Si/^{28}Si$ values for the same sets of grains. In both Figs. 7 and 8, the error-weighted least-squares fits to the combined measurements from all 4 datasets for mainstream grains are given by the solid lines, and the regression parameters are given in Table 1. Close inspection of Figs. 7 and 8 reveals some significant differences in the Ti compositions among the various datasets; therefore, in order to directly compare these apparent discrepancies, we have also calculated regression lines for the following three sets of mainstream grains (Table 1): the 220 grains measured in this study, data only from HAH, and the entire combined dataset of our data and HAH. The $\delta^{46}Ti/^{48}Ti$, $\delta^{47}Ti/^{48}Ti$, and $\delta^{49}Ti/^{48}Ti$ values measured here span ranges roughly from −150‰ up to a 200‰, whereas the $\delta^{50}Ti/^{48}Ti$ values can range up to 400‰. The Ti compositions reported here cover the previous data well, although with considerably more scatter and a larger spread. The $\delta^{46}Ti/^{48}Ti$ and $\delta^{47}Ti/^{48}Ti$ values (or equivalently the $^{46}Ti/^{48}Ti$ and $^{47}Ti/^{48}Ti$ ratios) agree very well with the previous data, and there is little difference in the correlation lines calculated for the different datasets. However, our data show larger isotopic enhancements, in general, for ^{49}Ti and ^{50}Ti relative to ^{48}Ti than previous measurements do. In addition, it can be seen in Fig. 7a that the degree of linearity determined from the correlation of $\delta^{50}Ti/^{48}Ti$ with $\delta^{46}Ti/^{48}Ti$ values from this study is substantially worse than that observed for the older datasets. The results here indicate little correlation among the grains' $\delta^{46}Ti/^{48}Ti$ and $\delta^{50}Ti/^{48}Ti$ values, as given by a reduced χ^2 value of 9.79,

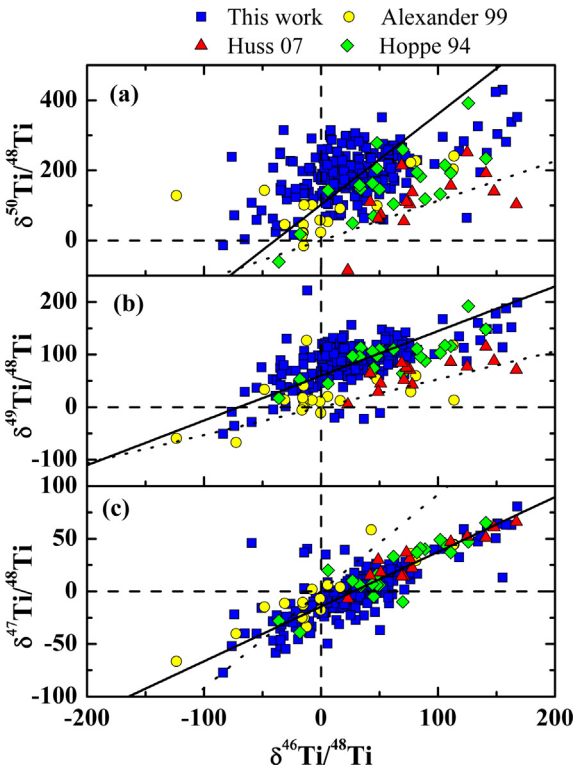

Fig. 7. Plot of the mainstream SiC Ti isotopic compositions of the present work compared with the data from Hoppe et al. (1994), Alexander and Nittler (1999), and Huss and Smith (2007). Also shown are the best fit lines to the combined datasets (solid lines) and the normalized GCE lines (dotted lines) from Timmes et al. (1995).

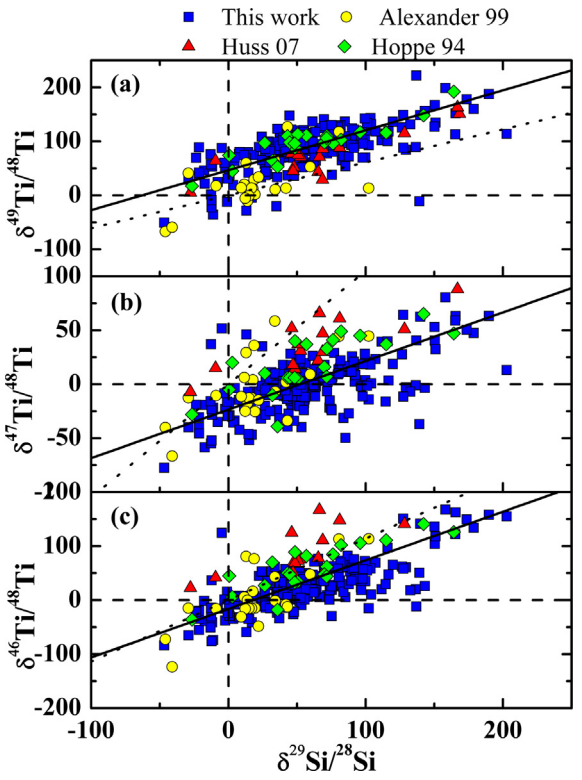

Fig. 8. Plot of $\delta^{46}Ti/^{48}Ti$, $\delta^{47}Ti/^{48}Ti$, and $\delta^{49}Ti/^{48}Ti$ values against $\delta^{29}Si/^{28}Si$ values of the present work compared with the data from Hoppe et al. (1994), Alexander and Nittler (1999), and Huss and Smith (2007). Also shown are the best fit lines to the combined datasets (solid lines) and the normalized GCE lines (dotted lines) from Timmes et al. (1995).

representative of a poor fit to the data, which tend to cluster around $\delta^{50}Ti/^{48}Ti \approx 200‰$. This is in contrast to the results for ^{50}Ti from the HAH dataset, which do exhibit a higher degree of linearity when plotted. The Si-Ti correlation lines through the new data are less steep than those derived from the previous analyses, similar to the Ti isotopes. These apparent discrepancies between the new data presented here and the previous datasets are most likely due to systematic differences between the different populations of SiC grains measured here and by previous authors. In the following discussion, possible explanations for these apparent observations will be given.

At least two scenarios can be envisaged which could possibly produce the elevated isotopic ratios (excepting $^{47}Ti/^{48}Ti$) shown by our data: perhaps for some unknown experimental reason during our measurements, the signal detected at mass 48 was under-counted or, alternatively, we over-corrected for the ^{48}Ca contribution to the 48 signal (which would happen if the grains had lower-than-solar $^{48}Ca/^{44}Ca$ ratios). However, for several reasons, we view any instrumental problem as unlikely. The strikingly good agreement of the $\delta^{46}Ti/^{48}Ti$ and $\delta^{47}Ti/^{48}Ti$ values with the previous data argues against any systematic problem with the mass 48 signal monitored here: if the ^{48}Ti signal were in any way too low (no matter the reason), it would also affect the $^{46}Ti/^{48}Ti$ and the $^{47}Ti/^{48}Ti$ ratios, which is, apparently, not the case. Furthermore, it would also produce excesses in ^{49}Ti and ^{50}Ti that would be very similar, which is also not observed. In addition, due to the instrumental setup chosen, ^{48}Ti (as well as ^{46}Ti) was actually measured on two different detectors. Comparisons of all Ti isotopic ratios (with ^{48}Ti in the denominator) derived from either detector monitored for mass 48 are virtually indistinguishable from each other, thereby eliminating the possibility that some instrumental artifact inadvertently reduced the sensitivity of one particular detector. Also, the Ti data presented here were taken in three separate measurement runs (separated by months), with 75 grains analyzed in each of the first two runs and the remaining 88 grains measured in a final run. If some unnoticed technical problem had affected a given measurement session, there is no reason, a priori, it should have affected the other two sessions, and would therefore produce a systematic difference in the data from session to session. However, no evidence for any such variability can be observed in our data. There is also little evidence for the grains having significantly lower-than-solar $^{48}Ca/^{44}Ca$ ratios: the correction applied is only about a few permil in this study and others (Huss and Smith, 2007; Zinner et al., 2007), AGB models do not predict ratios very different from solar, and the Ca/Ti ratios in the grains are at most a few percent, thereby reducing the uncertainty of the ^{46}Ca and ^{48}Ca corrections.

Alexander and Nittler (1999) saw such low Ca abundances that they did not even need to correct for Ca isobaric interferences at all.

It appears most likely, therefore, that the discrepancies between our data and the preexisting Ti data arise from the selection of grains chosen for study. As mentioned above, the grains measured by Alexander and Nittler (1999) and Hoppe et al. (1994) were not randomly chosen, but were selected based on high Ti contents or large Si isotopic anomalies, respectively. Therefore, these grains are not necessarily representative of the presolar SiC population as a whole. In Fig. 9, histograms of the $\delta^{29}Si/^{28}Si$ values of the various populations of grains analyzed for Ti isotopes are given. The Alexander and Nittler (1999) data are dominated (9 out of 20) by grains with $\delta^{29}Si/^{28}Si$ values between 10 and 20‰, while a substantial fraction of the grains from the other three datasets typically have $\delta^{29}Si/^{28}Si$ values between 40 and 60‰. For the ~10,000 mainstream grains with $\delta^{29}Si/^{28}Si$ and $\delta^{30}Si/^{28}Si$ errors less than 15‰ and 25‰, respectively (see appendix of Zinner et al., 2007), the mean $\delta^{29}Si/^{28}Si$ value is ~35‰, in much better agreement with the data from the grains measured here than with those from Hoppe et al. (1994) and from Huss and Smith (2007). It should be noted that, as remarked above, the grain data from this study are, on average, more enriched in ^{29}Si compared to the mainstream SiC population in general. In Fig. 7, it can be seen that for the Alexander and Nittler (1999) analyses, except for a few grains, the measured Ti isotopic ratios tend to cluster around solar compositions and, in fact, only 9 grains have Ti anomalies more than 2σ from solar for multiple isotopic ratios – five grains actually have no Ti isotopic anomalies more than 2σ away from solar compositions. Thus, it remains uncertain whether it is appropriate to directly compare the Alexander and Nittler (1999) data to the grain data presented here, in which over 90% of the grains have multiple Ti isotopic anomalies more than 2σ away from solar. The net effect of the data from Alexander and Nittler (1999) is to increase the slopes and decrease the intercepts of the Ti-Ti and Ti-Si correlation lines when these results are

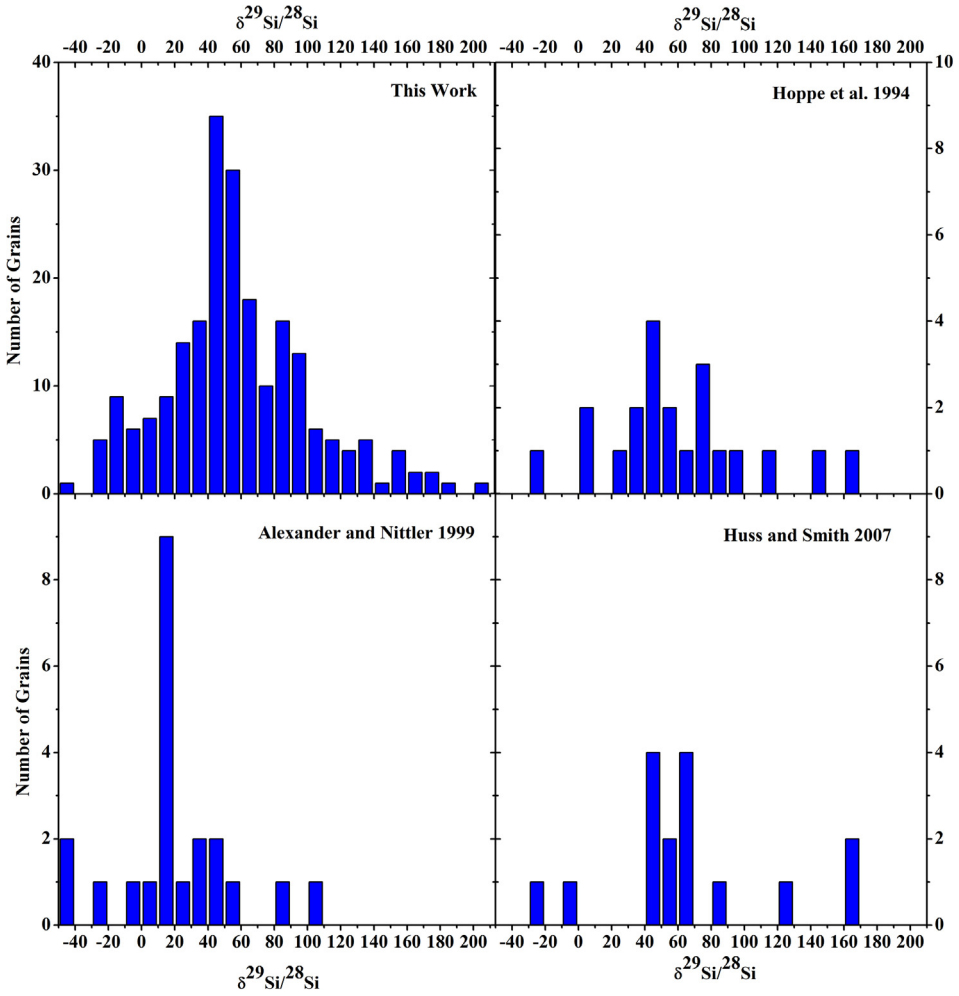

Fig. 9. Histogram of the $\delta^{29}Si/^{28}Si$ values for the 4 groups of mainstream presolar SiC grains measured for Ti from Hoppe et al. (1994), Alexander and Nittler (1999), Huss and Smith (2007), and the present work. Although the statistics are limited, the Alexander and Nittler (1999) data show that almost half of their grains have $\delta^{29}Si/^{28}Si$ values between 10 and 20‰, whereas for the other datasets a significant fraction of the grains analyzed have $\delta^{29}Si/^{28}Si$ values from 40 to 60‰.

combined with the Hoppe et al. (1994) and Huss and Smith (2007) data. If the Alexander and Nittler data are not considered, the results from the Hoppe et al. (1994) and Huss and Smith (2007) studies are in much better agreement with the present work, particularly for the $\delta^{49}Ti/^{48}Ti$ and $\delta^{50}Ti/^{48}Ti$ values. This can be seen in Fig. 7a and b, where the $\delta^{49}Ti/^{48}Ti$ and $\delta^{50}Ti/^{48}Ti$ values from Alexander and Nittler (1999) are significantly reduced compared to the other datasets and are much closer to zero. In addition, in Fig. 8a, it is puzzling why their grains have systematically lower $^{49}Ti/^{48}Ti$ ratios than grains with similar Si isotopic compositions from the other Ti studies. Overall, the data we have obtained seem to be in better agreement with the Hoppe et al. (1994) and Huss and Smith (2007) datasets, only with larger spread and variability, which is not entirely unexpected as we measured a larger and inherently more random set of grains. However, our data are somewhat above and below the Huss and Smith data in Fig. 7a, b and Fig. 8b, c, respectively.

The Ti isotopic compositions of the majority of mainstream SiC grains are typically observed to have $\delta^{47}Ti/^{48}Ti < \delta^{46}Ti/^{48}Ti < \delta^{49}Ti/^{48}Ti < \delta^{50}Ti/^{48}Ti$, consistent with n-capture nucleosynthesis in AGB stars. These isotopic compositions correspond to an asymmetric V-shape, when plotted as in Fig. 10, and this general trend has been observed in most of the grains from the Hoppe et al. (1994) and Huss and Smith (2007) studies. Depending on how the pattern is defined, roughly half of the mainstream SiC grains analyzed here exhibit this V-shaped isotopic signature, with the remaining grains displaying either irregular patterns (often with $\delta^{46}Ti/^{48}Ti < \delta^{47}Ti/^{48}Ti$) or inverted patterns (~1%, with $\delta^{46}Ti/^{48}Ti$, $\delta^{47}Ti/^{48}Ti$, $\delta^{49}Ti/^{48}Ti$, and $\delta^{50}Ti/^{48}Ti < 0$). As a large portion of grains from the Alexander and Nittler (1999) study do not have significant Ti anomalies in multiple isotopic ratios, it is not surprising that their grains do not show a V-shaped pattern. Again, this fundamental difference likely stems from the fact that the grains they analyzed are simply not as anomalous (in both Si and Ti) as the grains from Hoppe et al. (1994), Huss and Smith (2007), and the present work, making direct comparisons difficult.

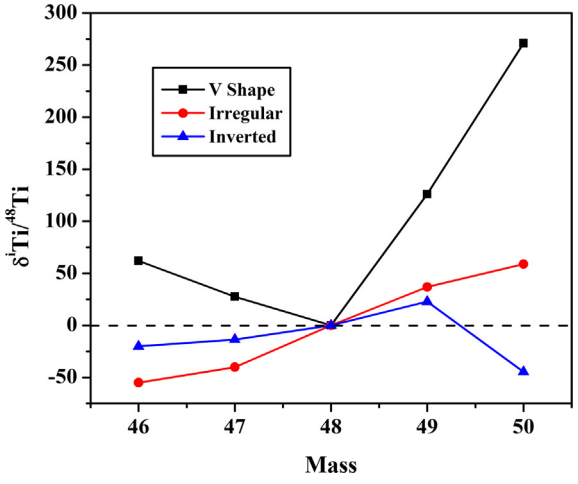

Fig. 10. Ti isotopic patterns typical of mainstream SiC grains from this study. Roughly half of the grains have V-shape patterns and inverted patterns are seen in ~1% of the grains.

4.4. Comparisons with AGB and GCE models

Thorough, comprehensive reviews of nucleosynthesis in AGB stars have been given by Busso et al. (1999) and Herwig (2005). Low-mass ($<3\ M_{\odot}$) AGB stars are radially stratified. The innermost region of these stars have a degenerate C-O core encompassed by two thin (in mass) concentric shells in which He-burning and H-burning can occur, separated only by a thin zone called the He intershell. Outside the H-burning shell is the extensive (and cooler) H-rich convective envelope. Minerals such as SiC can condense from the gaseous state at the star's surface and leave the star with the stellar wind. During the AGB phase, the star primarily burns H in the H-burning shell, the products of which (principally He) continually accrete onto the He intershell causing it to greatly increase in mass. Owing to partial degeneracy in the intershell, at high enough densities and temperatures a thermonuclear runaway occurs in which He-burning suddenly and dramatically ignites, resulting in a short thermal pulse (TP). The large energy produced by the TP (mainly through the triple-α reaction) interrupts the radiative state of the intershell, causing it to temporarily become convective and halt H shell burning (at least for a while). Following a TP and before the H-burning shell becomes active again, the bottom of the convective envelope penetrates into the top of the He intershell, which by nature of its temporary convection has become enriched in newly synthesized material from the bottom of the He-burning region. In this way, nuclearly processed material is dredged up (also known as a "third dredge-up episode", TDU) into the convective envelope, and the stellar surface becomes enriched in the ashes of He burning. As the TDU is a recurring event (from 10 to a 100 times), the envelope's composition becomes increasingly C-rich, eventually reaching $C/O > 1$, which is required for the condensation of SiC grains. The entire sequence described above has been termed the thermally pulsing asymptotic giant branch phase (TP-AGB).

Although extra mixing processes, such as cool bottom processing, may further modify isotopic compositions, low mass AGB stars do not reach temperatures great enough to ignite C burning, and thus neutron capture reactions are responsible for the production of the less abundant isotopes of Si and Ti. The dominant sources of free neutrons are two reactions which operate at different times in the He intershell: $^{13}C(\alpha,n)^{16}O$ and $^{22}Ne(\alpha,n)^{25}Mg$. The $^{13}C(\alpha,n)^{16}O$ reaction takes place at lower temperatures in between TPs (Straniero et al., 1997), resulting in low neutron density over a longer period of time than the $^{22}Ne(\alpha,n)^{25}Mg$ reaction, which only becomes active during the brief higher temperatures reached during a TP. The exact nature and origin of the ^{13}C-rich layer (^{13}C pocket), in which the $^{13}C(\alpha,n)^{16}O$ reaction operates, has been extensively debated (e.g., Herwig, 2005; Lattanzio and Lugaro, 2005; Straniero et al., 2006). Suffice to say, the ^{13}C pocket has essentially been treated as a free parameter in *s*-process calculations of AGB stars (Gallino et al., 1998)

by varying the pocket strength (up or down) relative to the nominal or standard ("ST" case) value required to best reproduce the *s*-process elemental abundances in the solar system (Gallino et al., 1997; Lugaro et al., 2003). Recently, a self-consistent mechanism for the natural formation of the ^{13}C pocket has been reported (Cristallo et al., 2009), in which the mass of ^{13}C in the pocket is found to decrease with subsequent TDU episodes, suggestive of a decrease in the efficiency of the *s*-process with time during the TP-AGB. Nevertheless, an increasing body of evidence, such as measurements of Ti (Zinner et al., 2007), Zr, Mo, and Ba (Barzyk et al., 2007; Marhas et al., 2007) in mainstream SiC grains and spectral observations of *s*-process enhanced elements in carbon stars (e.g., Abia et al., 2002), point to the adoption of a ^{13}C pocket at least close to the "ST" case. The neutrons required for production of the Ti isotopes primarily come from the ^{13}C source (Zinner et al., 2007), with only minor contributions from the ^{22}Ne source. In contrast, Si isotopic production is governed almost entirely by the flux of neutrons from the ^{22}Ne source, and large changes in the strength of the ^{13}C pocket have virtually negligible effects on the Si isotopic ratios (Lugaro et al., 1999; Zinner et al., 2006). Regardless, because of the small neutron capture cross-sections of the Ti (and Si) isotopes, they (except for ^{49}Ti and ^{50}Ti, due to the not-so-small cross-section of ^{48}Ti) are not significantly affected by n-capture. For mainstream SiC grains, thought to originate in close-to-solar metallicity AGB stars, the predicted shifts from n-capture (except for the magic-nucleus isotope ^{50}Ti) are small (Lugaro et al., 1999; Zinner et al., 2007); therefore, their Ti isotopic compositions largely contain the imprint of the initial composition of the grains' parent stars. The large spread of Ti isotopic compositions from the grains in this study further supports a wide distribution of initial stellar isotopic ratios.

Galactic chemical evolution (GCE) is the process by which elemental and isotopic abundances evolve over time in the Galaxy, and has been discussed in detail by many authors (Timmes et al., 1995; Nittler and Dauphas, 2006; Pagel, 2009). Briefly, homogeneous GCE assumes an age metallicity relationship, in that the ratios of secondary isotopes relative to a primary isotope of an element increase with time. Primary nuclei (e.g., ^{12}C, ^{16}O, ^{28}Si, ^{40}Ca, and radioactive ^{48}Cr, or alpha nuclei) can be created by stars whose initial compositions consist only of H and He and can therefore be synthesized at extremely low metallicity. In contrast, the creation of secondary nuclei (e.g., ^{46}Ti, ^{47}Ti, ^{49}Ti, and ^{50}Ti) requires the presence of seed elements heavier than H and He on which to capture a proton or neutron, thereby resulting in further nuclear processing (Clayton, 2003). As stars with low initial metallicity eject their nucleosynthesis products into the ISM at the end of their lives, the subsequent generations of stars will begin their lives forming from this newly processed material, will be more metal-rich, and, in turn, have more primary and secondary nuclei for nuclear burning. At the end of their lives, these stars eject their newly synthesized material, and this whole process of stellar recycling is repeated. In this way, as metallicity increases so do the ^{46}Ti/^{48}Ti, ^{47}Ti/^{48}Ti, ^{49}Ti/^{48}Ti, and ^{50}Ti/^{48}Ti ratios, as well as the ^{29}Si/^{28}Si and ^{30}Si/^{28}Si ratios.

Detailed models of GCE incorporating yields of Type II SNe show large increases of ^{29}Si, ^{30}Si, ^{46}Ti, ^{47}Ti, ^{49}Ti, and ^{50}Ti with galactic time and metallicity (Timmes et al., 1995) and have been extensively compared to the SiC grain data (Timmes and Clayton, 1996; Clayton and Timmes, 1997; Alexander and Nittler, 1999; Huss and Smith, 2007; Zinner et al., 2007). As discussed by these authors, problems with directly comparing the predictions of Timmes et al. (1995) to the Si and Ti compositions of the grains remain, as can be seen in Figs. 7 and 8 showing the mainstream correlation lines to the combined datasets (solid lines) and the calculated GCE lines (dotted lines) from Timmes et al. (1995), which have been normalized to have solar ratios at solar metallicity. It should be noted that the Timmes et al. (1995) GCE model actually under produces ^{47}Ti and ^{50}Ti and overproduces ^{46}Ti by up to a factor of three; the un-normalized GCE lines would not fit on the plots in Figs. 7 and 8. The best fits to the mainstream SiC grain data, which are largely representative of the compositions of the grains' parent stars, are significantly different from the GCE trends (Table 1), even if corrected for contributions from AGB nucleosynthesis, which are substantial for ^{49}Ti and ^{50}Ti. It has been suggested that a component of heterogeneous GCE could account for the spread in the grain data and the discrepancies with GCE trends (Lugaro et al., 1999) for the Si isotopes. However, more detailed calculations for the isotopic compositions of other elements, especially Ti, failed to reproduce the Si-Ti correlation observed in the SiC grain data, thereby limiting the amount of stochastic mixing of SN ejecta (the dominant component in GCE) into the ISM (Nittler, 2005).

As alluded to above, the large spread in Ti (and Si) isotopic ratios of mainstream, type Y and type Z presolar SiC grains must be due to a combination of the initial compositions of the parent stars and n-capture during the TP-AGB phase. It is possible, therefore, that with stellar evolution models for AGB stars of different masses and metallicities, the nucleosynthesis component can be separated from the GCE effect – see Fig. 11 in Zinner et al. (2007) – and thus, the evolution of the initial Si and Ti isotopic ratios of the grains can be determined as a function of metallicity, essentially from the grain data and AGB models alone. For the Si isotopes, this procedure was first outlined by Amari et al. (2001a) and Zinner et al. (2001), and has been updated to include new AGB model calculations, a larger grain dataset, and updated nuclear cross-sections (Zinner et al., 2006). It is typically performed by assuming that the best-fit line to the mainstream SiC data – some authors correct this line for AGB contributions, while others prefer not to – represents the Galactic evolution line. Isotopic shifts away from this line are interpreted to be from AGB nucleosynthesis, along a slope ~0.18 line in a three-isotope δ-value Si plot for models calculated with n-capture cross-sections from Guber et al. (2003). For a given isotopic composition, the isotopic ratios are extrapolated back along this AGB line to the point of intersection with the mainstream correlation line, from which the shifts due to

n-capture, defined as $\Delta^{29}Si/^{28}Si$ and $\Delta^{30}Si/^{28}Si$ values, as well as, the initial $\delta^{29}Si/^{28}Si$ value of the grain's parent star can be calculated. There are some fundamental uncertainties involved in this routine: the grains must be assumed to come from stars of the same mass but with varying metallicities and the shifts in the isotopic compositions due to n-capture are derived from model calculations. The initial masses of the presolar SiC grains' parent stars are not well constrained and are estimated to range from 1.5 to 3 $M_{\odot}$, in contrast to presolar oxides, where the mass of the progenitor stars can be fairly precisely determined due to the strong coupling between the $^{17}O/^{16}O$ ratios produced from first dredge-up and the initial stellar mass (Boothroyd and Sackmann, 1999). As most of the *s*-process enhancements in the envelope are primarily due to the first few TDU episodes (Cristallo et al., 2009) and most SiC have likely formed after a significant number of TPs when the star has turned into a carbon star (Lugaro et al., 2003), assuming maximum isotopic shifts from n-capture is at least approximately valid. *S*-process elements continue to be enhanced after each thermal pulse; as the convective envelope is losing mass, even a small amount of *s*-processed material dredged-up will enhance the concentration of *s*-process elements, but not to significant amounts. Despite these caveats, the initial $^{29}Si/^{28}Si$ ratios – see Fig. 15 of Zinner et al. (2006) – for type Z grains as a function of metallicity can be determined for a given initial stellar mass, and is significantly different than the Timmes and Clayton (1996) Si GCE line. The evolution of the initial $\delta^{29}Si/^{28}Si$ values calculated from the grain data shows enrichments in ^{29}Si at very low metallicity (as well a significantly flatter trend at $Z > 0.01$) compared to the Timmes and Clayton results (1996), and suggests modifications in the yields of ^{29}Si and ^{28}Si from low-metallicity Type II SNe and increased contributions of ^{28}Si from Type Ia SNe occurring from close binary star systems (Zinner et al., 2006).

In principle, the Ti isotopic compositions of presolar SiC grains from AGB stars can be deconvolved into the isotopic shifts due to AGB nucleosynthesis and the initial compositions of the grains' parent stars, as attempted by several authors (Alexander and Nittler, 1999; Amari et al., 2001a; Huss and Smith, 2007); however, the situation for the Ti isotopes is not as straightforward as for the Si isotopes. While Alexander and Nittler (1999) and Amari et al. (2001a) essentially subtracted the average predicted AGB contribution from the best-fit line to the mainstream grains Ti isotopic compositions, Huss and Smith (2007) scaled this contribution to the shift due to n-capture calculated for the Si isotopes to infer the Galactic evolution line for the Ti isotopes. However, there are several intrinsic problems with applying this approach to the Ti isotopes. Because Ti is a trace element in presolar SiC grains, their measured Ti isotopic ratios have significantly larger errors and show more scatter around the mainstream correlation lines than the Si isotopic data. Nevertheless, the weak correlations for the $^{46}Ti/^{48}Ti$ – $^{49}Ti/^{48}Ti$ and $^{46}Ti/^{48}Ti$ – $^{50}Ti/^{48}Ti$ ratios are not solely the result of measurement errors, but, in fact, represent intrinsic differences between the contributions from AGB nucleosynthesis and GCE in the grains' parent stars. In fact, the best-fit lines themselves (for any combination of Ti and/or Si δ-values) are not well established, as there are significant differences among the best-fits lines for the different sets of grains analyzed for Ti isotopes (Table 1). In addition, model predictions of nucleosynthesis of the Ti isotopes in AGB stars are fundamentally less certain than for Si. Unlike the Si isotopes, which are primarily affected by the neutrons from the ^{22}Ne source, the production of the secondary Ti isotopes depends on the strength of the ^{13}C pocket, which is essentially a free parameter, and is intrinsically uncertain. It has been shown by both Zinner et al. (2007) and Huss and Smith (2007) that the while AGB models computed for the ST pocket provide consistent inferred $\delta^{46}Ti/^{48}Ti$ values, they overproduce ^{49}Ti and ^{50}Ti relative to the grain data. Therefore, the strength of the ^{13}C pocket must depend in some as yet unknown way on the metallicity of the star, and further refinements of the model calculations are clearly needed. With heavier metallicity, metals act as n-poisons, but for lower metallicity, one predicts higher enrichments on n-rich isotopes. As is the case for the deconvolution procedure for the Si isotopes, the precise range of masses and metallicities of the grains' parent stars is unknown, further complicating any AGB correction. In addition, as only 4 type Y and 4 type Z grains were measured in this study, we do not have enough data for grains from low metallicity stars and, therefore, will not attempt to directly calculate the Galactic evolution lines of the Ti isotopes. A larger number of type Z grains need to be measured with small analytical uncertainties and the parameter space of the AGB models needs to be better explored to infer the initial Ti isotopic compositions of the SiC grains' parent stars as a function of metallicity and explain the grain data.

As can be seen in Table 1, the inferred slopes of the GCE lines calculated by Timmes et al. (1995) fail to match the error-weighted linear regressions for the mainstream SiC data. However, as the mainstream correlation lines represent a combination of both GCE and n-capture nucleosynthesis, these fits are only approximate estimates of the galactic evolution of the Ti isotopes, in particular, for ^{49}Ti and ^{50}Ti. The grain data show steeper trendlines for the $\delta^{49}Ti/^{48}Ti$ vs. $\delta^{46}Ti/^{48}Ti$ and $\delta^{50}Ti/^{48}Ti$ vs. $\delta^{46}Ti/^{48}Ti$ plots than predicted by Timmes et al. (1995), while the $\delta^{47}Ti/^{48}Ti$ vs. $\delta^{46}Ti/^{48}Ti$ plot shows a much shallower slope (Fig. 7). The production of ^{47}Ti is poorly understood and is under-produced in SN models relative to its solar system abundance, so it is not surprising that its evolution does not agree particularly well with the grain data. The greatest discrepancy between the grain data and the Timmes et al. (1995) results can be seen in the $\delta^{50}Ti/^{48}Ti$ vs. $\delta^{46}Ti/^{48}Ti$ plot, where the mainstream correlation line is more than twice as steep as the trend from GCE; however, the large scatter in the $^{50}Ti/^{48}Ti$ ratios in the grain data implies that the linear fit is of limited statistical significance. This scatter is likely due to the fact that ^{50}Ti is principally produced in Type Ia SNe (Meyer et al., 1996), which are prodigious generators of n-rich isotopes but are extremely rare. Stars ending in Type Ia SNe evolve much more slowly than the more massive ones ending in Type II SNe (the dominant source for the other Ti isotopes), thus their contribution to the

GCE of Ti is more important at later galactic times, resulting in a more heterogeneous distribution of ^{50}Ti (Zinner et al., 2007). It should be noted that ^{50}Ti is also produced by nuclear statistical equilibrium in Type II SNe. Similarly for the Si-Ti correlation lines, the GCE models do not generally match the trends seen for the grain data, although there is fairly good agreement in the $\delta^{49}Ti/^{48}Ti$ vs. $\delta^{29}Si/^{28}Si$ correlation lines.

5. CONCLUSION

The C, N, Si, and Ti isotopic compositions of 238 presolar SiC grains from the Murchison meteorite have been determined, almost doubling the number of SiC grains analyzed for Ti isotopes. The Si isotopic compositions of the KJG SiC grains measured here and previously are characterized by greater $\delta^{29}Si/^{28}Si/\delta^{30}Si/^{28}Si$ ratios than the majority of other mainstream SiC grains. We have suggested that this result may reflect a subtle dilution from marginal type Y and Z grains in the larger dataset, and perhaps the "true" mainstream correlation line for the Si isotopes is steeper than previously thought. The Ti isotopic compositions of the grains have been shown to span those of previous measurements. By attempting to measure as random a population of grains as possible, the range and spread of the Ti isotopic ratios measured in presolar SiC grains has been greatly increased. Still, it is clear that the grains' Si and Ti isotopic compositions represent a combination of GCE and n-capture in the grains' parent stars, in contrast to spectroscopic measurements of Ti isotopic compositions in M dwarf stars. The large dataset of this work, combined with the monitoring of the ^{51}V signal, leads us to conclude that Ti must be present in the majority of SiC grains as discrete subgrains and not in solid solution. Deconvolving the GCE and AGB components of Ti from the grain data will require more high precision Ti data on SiC grains from low-metallicity stars, such as type Y and Z grains, and new model calculations for AGB stars starting from a wide range of initial Ti isotopic ratios and for a range of Ti isotope n-capture cross-sections. Unfortunately, as the abundance of type Z grains is significantly lower among grains with diameters greater than ~1 μm than among smaller grains, obtaining high quality Ti isotopic data with small errors for a large number of these grains will be difficult.

ACKNOWLEDGMENTS

This paper is dedicated with love to our dear friend and colleague Ernst Zinner. Without his help – scientific, instrumental, and personal – this work would not have been possible. We thank Tim Smolar for his relentless effort in maintaining the NanoSIMS and Tom Bernatowicz and K. Mairin Hynes for useful discussions. We thank Roy Lewis for providing the KJG samples and NASA for financial support though grants NNX08AG71G and NNX11AH14G to EZ.

APPENDIX A. SUPPLEMENTARY MATERIAL

Supplementary data associated with this article can be found, in the online version, at https://doi.org/10.1016/j.gca.2017.09.031.

REFERENCES

Abia C., Domínguez I., Gallino R., Busso M., Masera S., Straniero O., de Laverny P., Plez B. and Isern J. (2002) *S*-Process nucleosynthesis in carbon stars. *Astrophys. J.* **579**, 817–831.

Alexander C. M. O. D. and Nittler L. R. (1999) The galactic evolution of Si, Ti and O isotopic ratios. *Astrophys. J.* **519**, 222–235.

Amari S., Hoppe P., Zinner E. and Lewis R. S. (1995) Trace-element concentrations in single circumstellar silicon carbide grains from the Murchison meteorite. *Meteoritics* **30**, 679–693.

Amari S., Lewis R. S. and Anders E. (1994) Interstellar grains in meteorites: I. Isolation of SiC, graphite, and diamond; size distributions of SiC and graphite. *Geochim. Cosmochim. Acta* **58**, 459–470.

Amari S., Nittler L. R., Zinner E., Gallino R., Lugaro M. and Lewis R. S. (2001a) Presolar SiC grains of type Y: origin from low-metallicity asymptotic giant branch stars. *Astrophys. J.* **546**, 248–266.

Amari S., Nittler L. R., Zinner E., Lodders K. and Lewis R. S. (2001b) Presolar SiC grains of type A and B: their isotopic compositions and stellar origins. *Astrophys. J.* **559**, 463–483.

Amari S., Zinner E. and Lewis R. S. (2000) Isotopic compositions of different presolar silicon carbide size fractions from the Murchison meteorite. *Meteorit. Planet. Sci.* **35**, 997–1014.

Barzyk J. G., Savina M. R., Davis A. M., Gallino R., Gyngard F., Amari S., Zinner E., Pellin M. J., Lewis R. S. and Clayton R. N. (2007) Constraining the ^{13}C neutron source in AGB stars through isotopic analysis of trace elements in presolar SiC. *Meteorit. Planet. Sci.* **42**, 1103–1119.

Bernatowicz T. J., Amari S. and Lewis R. S. (1992) TEM studies of a circumstellar rock. *Lunar Planet. Sci. XXIII*, 91–92.

Bernatowicz T. J., Cowsik R., Gibbons P. C., Lodders K., Fegley, , B., Amari S. and Lewis R. S. (1996) Constraints on stellar grain formation from presolar graphite in the Murchison meteorite. *Astrophys. J.* **472**, 760–782.

Besmehn A. and Hoppe P. (2003) A NanoSIMS study of Si- and Ca-Ti-isotopic compositions of presolar silicon carbide grains from supernovae. *Geochim. Cosmochim. Acta* **67**, 4693–4703.

Boothroyd A. I. and Sackmann I.-J. (1999) The CNO isotopes: deep circulation in red giants and first and second dredge-up. *Astrophys. J.* **510**, 232–250.

Busso M., Gallino R. and Wasserburg G. J. (1999) Nucleosynthesis in asymptotic giant branch stars: relevance for Galactic enrichment and solar system formation. *Ann. Rev. Astron. Astrophys.* **37**, 239–309.

Clayton D. (2003) Handbook of Isotopes in the Cosmos.

Clayton D. D. and Timmes F. X. (1997) Implications of presolar grains for galactic chemical evolution. In *Astrophysical Implications of the Laboratory Study of Presolar Materials* (eds. T. J. Bernatowicz and E. Zinner). AIP, New York, pp. 237–264.

Cristallo S., Straniero O., Gallino R., Piersanti L., Domínguez I. and Lederer M. T. (2009) Evolution, nucleosynthesis, and yields of low-mass asymptotic giant branch stars at different metallicities. *Astrophys. J.* **696**, 797–820.

Croat T. K., Staderman F. J. and Bernatowicz T. J. (2010) Unusual ^{29,30}Si-rich SiCs of massive star origin found within graphites from the Murchison meteorite. *Astronom. J.* **139**, 2159–2169.

Croat T. K., Bernatowicz T., Amari S., Messenger S. and Stadermann F. J. (2003) Structural, chemical, and isotopic microanalytical investigations of graphite from supernovae. *Geochim. Cosmochim. Acta* **67**, 4705–4725.

Ebel D. S. (2006) Condensation of rocky material in astrophysical environments. In *Meteorites and the Early Solarstem II* (eds. D. S. Lauretta and H. Y. McSween). University of Arizona Press, Tucson, pp. 253–277.

Gallino R., Arlandini C., Busso M., Lugaro M., Travaglio C., Straniero O., Chieffi A. and Limongi M. (1998) Evolution and nucleosynthesis in low-mass asymptotic giant branch stars. II. Neutron capture and the *s*-process. *Astrophys. J.* **497**, 388–403.

Gallino R., Busso M. and Lugaro M. (1997) Neutron capture nucleosynthesis in AGB stars. In *Astrophysical Implications of the Laboratory Study of Presolar Materials* (eds. T. J. Berrnatowicz and E. Zinner). AIP, New York, pp. 115–153.

Guber K. H., Koehler P. E., Derrien H., Valentine T. E., Leal L. C., Sayer R. O. and Rauscher T. (2003) Neutron capture reaction rates for silicon and their impact on the origin of presolar mainstream SiC grains. *Phys. Rev. C* **67**, 62802–62804.

Gyngard F., Amari S., Jadhav M., Marhas K., Zinner E. and Lewis R. S. (2006a) Titanium isotopic ratios in KJG presolar SiC grains from Murchison. *Meteorit. Planet. Sci.* **41**, A71.

Gyngard F., Amari S., Jadhav M., Zinner E. and Lewis R. S. (2006b) Carbon, nitrogen, and silicon isotopic ratios in KJG presolar SiC grains from Murchison. *Lunar Planet. Sci.* **XXXVII**. Abstract #2194.

Herwig F. (2005) Evolution of asymptotic giant branch stars. *Ann. Rev. Astron. Astrophys.* **43**, 435–479.

Hinton R. W. (1990) Ion microprobe trace-element analysis of silicates: measurement of multi-element glasses. *Chem. Geol.* **83**, 11–25.

Hoppe P., Fujiya W. and Zinner E. (2012) Sulfur molecule chemistry in supernova ejecta recorded by silicon carbide stardust. *Astrophys. J.L.* **745**, 26–31.

Hoppe P., Amari S., Zinner E., Ireland T. and Lewis R. S. (1994) Carbon, nitrogen, magnesium, silicon and titanium isotopic compositions of single interstellar silicon carbide grains from the Murchison carbonaceous chondrite. *Astrophys. J.* **430**, 870–890.

Hoppe P. and Ott U. (1997) Mainstream silicon carbide grains from meteorites. In *Astrophysical Implications of the Laboratory Study of Presolar Materials* (eds. T. J. Bernatowicz and E. Zinner). AIP, New York, pp. 237–264.

Hoppe P., Strebel R., Eberhardt P., Amari S. and Lewis R. S. (1996) Small SiC grains and a nitride grain of circumstellar origin from the Murchison meteorite: implications for stellar evolution and nucleosynthesis. *Geochim. Cosmochim. Acta* **60**, 883–907.

Huss G. R. and Smith J. B. (2007) Titanium isotopic compositions of well-characterized silicon carbide grains from Orgueil (CI): Implications for *s*-process nucleosynthesis. *Meteor. Planet. Sci.* **42**, 1055–1075.

Hynes K. M. and Gyngard F. (2009) The presolar grain database. *Lunar Planet. Sci.* **40**, 1198, <http://presolar.wustl.edu/Laboratory_for_Space_Sciences/Presolar_Grain_Database.html>.

Ireland T. R., Zinner E. K. and Amari S. (1991) Isotopically anomalous Ti in presolar SiC from the Murchison meteorite. *Astrophys. J.* **376**, L53–L56.

Jacobsen B., Yin Q., Moynier F., Amelin Y., Krot A. N., Nagashima K., Hutcheon I. D. and Palme H. (2008) ^{26}Al-^{26}Mg and ^{207}Pb-^{206}Pb systematics of Allende CAIs: canonical solar initial ^{26}Al/^{27}Al ratio reinstated. *Earth Planet. Sci. Lett.* **272**, 353–364.

José J. and Hernanz M. (2007) The origin of presolar nova grains. *Meteorit. Planet. Sci.* **42**, 1135–1143.

Lattanzio J. C. and Lugaro M. A. (2005) What we *do* and *do not* know about the *s*-process in AGB stars. *Nucl. Phys. A* **758**, 477c–484c.

Lodders K. (2003) Solar system abundances and condensation temperatures of the elements. *Astrophys. J.* **591**, 1220–1247.

Lodders K. and Fegley, Jr., B. (1995) The origin of circumstellar silicon carbide grains found in meteorites. *Meteoritics* **30**, 661–678.

Lugaro M., Davis A. M., Gallino R., Pellin M. J., Straniero O. and Käppeler F. (2003) Isotopic compositions of strontium, zirconium, molybdenum, and barium in single presolar SiC grains and asymptotic giant branch stars. *Astrophys. J.* **593**, 486–508.

Lugaro M., Zinner E., Gallino R. and Amari S. (1999) Si isotopic ratios in mainstream presolar SiC grains revisited. *Astrophys. J.* **527**, 369–394.

Marhas K. K., Hoppe P. and Ott U. (2007) NanoSIMS studies of Ba isotopic compositions in single presolar silicon carbide grains from AGB stars and supernovae. *Meteorit. Planet. Sci.* **42**, 1077–1101.

McSween H. Y. and Huss G. R. (2010) *Cosmochemistry*. Cambridge University Press, New York.

Meyer B. S., Krishnan T. D. and Clayton D. D. (1996) ^{48}Ca production in matter expanding from high temperature and density. *Astrophys. J.* **462**, 825–838.

Nittler L. R. (2005) Constraints on heterogeneous galactic chemical evolution from meteoritic stardust. *Astrophys. J.* **618**, 281–296.

Nittler L. R. and Alexander C. M. O. D. (2003) Automated isotopic measurements of micron-sized dust: application to meteoritic presolar silicon carbide. *Geochim. Cosmochim. Acta* **67**, 4961–4980.

Nittler L. R. and Ciesla F. (2016) Astrophysics with extraterrestrial materials. *Ann. Rev. Astron. Astrophys.* **54**, 53–93.

Nittler L. R. and Dauphas N. (2006) Meteorites and the chemical evolution of the Milky Way. In *Meteorites and the Early Solar System II* (eds. D. S. Lauretta and , Jr.H. Y. McSween). Univ. of Arizona, Tucson, pp. 127–146.

Pagel B. E. J. (2009) *Nucleosynthesis and Chemical Evolution of Galaxies*, second ed. Cambridge Univ. Press, Cambridge.

Rocholl A. B. E., Simon K., Jochum K. P., Bruhn F., Gehan R., Kramar U., Luecke W., Molazan M., Pernicka E., Seufert M. and Stummier J. (1997) Chemical characteristics of NIST silicate reference material SRM 610 by ICP-MS, LIMS, SSMS, INAA, AAS and PIXE. *Geostandards Newslett.: J. Geostandards Geoanal.* **21**, 101–114.

Straniero O., Chieffi A., Limongi M., Busso M., Gallino R. and Arlandini C. (1997) Evolution and nucleosynthesis in low-mass asymptotic giant branch stars. I. Formation of population I carbon stars. *Astrophys. J.* **478**, 332–339.

Straniero O., Gallino R. and Cristallo S. (2006) S process in low-mass asymptotic giant branch stars. *Nucl. Phys. A* **777**, 311–339.

Stroud R. M. and Bernatowicz T. J. (2005) Surface and internal structure of pristine presolar silicon carbide. *Lunar Planet. Sci.* **XXXVI**. Abstract #2010.

Timmes F. X. and Clayton D. D. (1996) Galactic evolution of silicon isotopes: application to presolar SiC grains from meteorites. *Astrophys. J.* **472**, 723–741.

Timmes F. X., Woosley S. E. and Weaver T. A. (1995) Galactic chemical evolution: hydrogen through zinc. *Astrophys. J. Suppl.* **98**, 617–658.

Virag A., Wopenka B., Amari S., Zinner E., Anders E. and Lewis R. S. (1992) Isotopic, optical, and trace element properties of large single SiC grains from the Murchison meteorite. *Geochim. Cosmochim. Acta* **56**, 1715–1733.

Zinner E. (2007) Presolar Grains. In *Treatise on Geochemistry* (eds. D. H. Heinrich and K. T. Karl). Pergamon, Oxford, pp. 1–33.

Zinner E., Amari S., Gallino R. and Lugaro M. (2001) Evidence for a range of metallicities in the parent stars of presolar SiC grains. *Nucl. Phys. A* **688**, 102–105.

Zinner E., Amari S., Guinness R., Jennings C., Mertz A. F., Nguyen A. N., Gallino R., Hoppe P., Lugaro M., Nittler L. R. and Lewis R. S. (2007) NanoSIMS isotopic analysis of small presolar grains: search for Si_3N_4 grains from AGB stars, and Al

and Ti isotopic compositions of rare presolar SiC grains. *Geochem. Cosmochim. Acta* **71**, 4786–4813.

Zinner E., Nittler L. R., Gallino R., Karakas A. I., Lugaro M., Straniero O. and Lattanzio J. C. (2006) Silicon and carbon isotopic ratios in AGB stars: SiC grain data, models, and the galactic evolution of the Si isotopes. *Astrophys. J.* **650**, 350–373.

Associate editor: Anders Meibom